

# Bearingless Permanent Magnet Synchronous Motor using Independent Control

*By* Tole Sutikno

## Bearingless Permanent Magnet Synchronous Motor using Independent Control

Normaisharah Mamat<sup>1</sup>, Kasrul Abdul Karim<sup>2</sup>, Zulkiflie Ibrahim<sup>3</sup>, Tole Sutikno<sup>4</sup>

10 Siti Azura Ahmad Tarusan<sup>5</sup>, Auzani Jidin<sup>6</sup>

<sup>1,2,3,5,6</sup>Department of Electrical Engineering, Universiti Teknikal Malaysia Melaka, Malacca, Malaysia

<sup>4</sup>Department of Electrical Engineering, Universitas Ahmad Dahlan, Yogyakarta, Indonesia

### Article Info

#### Article history:

Received Mar 13, 2015

Revised Apr 28, 2015

Accepted May 15, 2015

#### Keyword:

Bearingless motor

Finite Element Method

Mathematical model

Permanent magnet synchronous motor

Self-bearing

### ABSTRACT

Bearingless permanent magnet synchronous motor (BPMSM) combines the characteristic of the conventional permanent magnet synchronous motor and magnetic bearing in one electric motor. BPMSM is a kind of high performance motor due to having both advantages of PMSM and magnetic bearing with simple structure, high efficiency, and reasonable cost. The research on BPMSM is to design and analyse BPMSM by using Maxwell 2-Dimensional of ANSYS Finite Element Method (FEM). Independent suspension force model and bearingless PMSM model are developed by using the method of suspension force. Then, the mathematical model of electromagnetic torque and radial suspension force has been developed by using Matlab/Simulink. The relation between force, current, distance and other parameter are determined. This research covered the principle of suspension force, the mathematical model, FEM analysis and digital control system of bearingless PMSM. This kind of motor is widely used in high speed application such as compressors, pumps and turbines.

Copyright © 2015 Institute of Advanced Engineering and Science.  
All rights reserved.

### Corresponding Author:

Normaisharah binti Mamat @ Mohd Nor,  
Departement of Electrical Engineering,  
Universiti Teknikal Malaysia Melaka (UTeM),  
76100 Durian Tunggal, Malacca, Malaysia.  
Email: normysarahmn@gmail.com

## 1. INTRODUCTION

The bearingless motor is the combination between magnetic bearings and electric motors in one system. Magnetic bearing is used to suspend a rotor without any mechanical contact by using magnetic levitation force and has the characteristic such as no wear, no lubricant, no friction, long life operating life and high precision. The problem on using magnetic bearing is in rotating the rotor because there is an additional motor element must be installed which makes the magnetic bearing system becomes a complicated structure and large size of system due to the long axial length of the rotor shaft. Thus the solution to overcome this problem is use the bearingless motor where is the motor will combine the generation of torque and magnetic suspension in one motor [1].

Bearingless motor was used for the first time by R. Bosch in 1988. Bearingless motor does not mean the lack of bearing forces but it means of the missing of physical contact bearing components. The principle of bearingless motor is based on the contactless magnetic bearing of rotor [2]. In order to suspend the rotor the principle of radial suspension force is studied. Two sets of winding are embedded at the same stator slot called motoring torque winding and radial suspension force winding. The suspension force winding makes the magnetic field in air gap becomes unbalanced and electromagnetic torque and radial suspension force are generated. To obtain the stable rotor the mathematical model is developed to make sure the position of rotor do not touch the inner stator [3].

Bearingless motor have been researched nowadays due to a lot of advantages. The example of bearingless motors that have been developed nowadays are bearingless switched reluctance motors, bearingless induction motor, bearingless brushless DC motors and bearingless permanent magnet synchronous motor (PMSM) [1]. However in this paper, bearingless surface mount PMSM has been focused and studied. Most researchers use surface mount permanent magnet compared to surface inset because the permeability of permanent magnet is close to the air due to the permanent magnet is mounted on the rotor surface. This paper will discuss the principle of suspension method, mathematical model, FEM analysis, independent suspension control and control system of BPMSM.

## 2. SUSPENSION FORCE PRINCIPLE

Bearingless motor can be realized by generating an active controllable magnetic field in the motor airgap. To ensure the rotor is manageably suspended under the action of magnetic forces, the interaction of suspension force winding and torque winding with airgap magnetic field must be generated. The generation of torque and suspension force at the same time is occurred when the torque winding and suspension force winding are placed in the same stator slots [3]. In order to produce controllable suspension forces, the pole pairs relationship between torque winding and suspension winding should meet the condition of  $P_M = P_B \pm 1$ , where  $P_M$  and  $P_B$  are referred to pole pair number for torque winding and suspension winding respectively. Based on the Figure 1, the torque windings,  $N_a$  and  $N_b$  have pole pairs of 2 respectively while  $N_x$  and  $N_y$  which are suspension force winding have pole pairs of 1. When the rotor displacement is at the centre with no current flowing in  $N_x$  and  $N_y$ , the resulting of symmetrical 4-pole flux  $\Phi_p$  is produced, flux density in each airgap is equal and no suspension force is produced. The rotor displacement at the negative direction of x-axis causes positive Maxwell-Force is generated to oppose the changes.

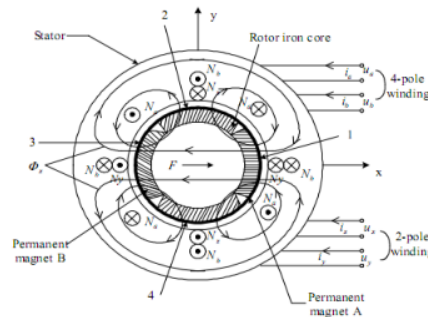


Figure 1. Principle of radial force production [4]

To ensure the rotor is in the centred position, the magnetic flux in area marked by 1 and 2 is regulated. The positive current of suspension winding  $N_x$  will cause the 2-pole fluxes  $\Phi_x$  are generated and flux density in the airgap area 2 is increased while the flux in area 1 is decreased. To make the rotor returns to the central position, negative direction force of x-axis must be produced. The same principle applied if the rotor is moving towards negative x-axis which causes the current of suspension winding becomes negative [4], [5].

## 3. RESEARCH METHOD

### 3.1. Mathematical model

This part presents the equations that used in designing BPMSM based on the paper [3]-[7]. Based on the electromagnetic field theory, when the rotor is out of the center another radial force will exist. It generates Maxwell force,  $F_{sx}$  and  $F_{sy}$  which applied on the rotor [4]. This force is proportion to the off center displacement and inherent forces written as (1) where  $k_s$  = force displacement coefficient

$$\begin{aligned} F_{sx} &= k_s x \\ F_{sy} &= k_s y \end{aligned} \quad (1)$$

The mathematical model for flux linkage and current of suspension force winding is written in (2) by expressed in the component of 2-phase  $d$ - $q$  axis.  $K_M$  and  $K_L$  are Maxwell force and Lore [16] force constant respectively.  $\Psi_{md}$  and  $\Psi_{mq}$  are airgap flux linkage in  $d$ - $q$  axis and  $i_{sd}$  and  $i_{sq}$  are current of the suspension force in  $d$ - $q$  axis.

$$\begin{bmatrix} F_{ix} \\ F_{iy} \end{bmatrix} = (K_M \pm K_L) \begin{bmatrix} \Psi_{md} & \Psi_{mq} \\ -\Psi_{mq} & \Psi_{md} \end{bmatrix} \begin{bmatrix} i_{sd} \\ i_{sq} \end{bmatrix} \quad (2)$$

To obtain the radial force for the direction at  $x$  and  $y$  axis, the equation (1) and (2) are combined to produce radial suspension force as shown in equation (3)

$$\begin{bmatrix} F_x \\ F_y \end{bmatrix} = (K_M + K_L) \begin{bmatrix} \Psi_{md} & \Psi_{mq} \\ \Psi_{mq} & \Psi_{md} \end{bmatrix} \begin{bmatrix} i_{sd} \\ i_{sq} \end{bmatrix} + k_s \begin{bmatrix} x \\ y \end{bmatrix} \quad (3)$$

The other equation to transform the radial force into current form is derived as below. The equation is developed in matrix form for flux linkage and current for both torque and suspension winding.  $N_\alpha$  and  $N_\beta$  such as shown in Figure 1 are defined as flux linkage of  $\Psi_{m\alpha}$  and  $\Psi_{m\beta}$  while  $N_x$  and  $N_y$  are defined as  $\Psi_{s\alpha}$  and  $\Psi_{s\beta}$ .  $L_m$  and  $L_B$  are self-inductance for motor winding and suspension force winding respectively.  $M'$  is mutual inductance.  $i_{s\alpha}$  and  $i_{s\beta}$  refer to  $\alpha$ -axis component and  $\beta$ -axis component of suspension force windings.

$$\begin{bmatrix} \Psi_{m\alpha} \\ \Psi_{m\beta} \\ \Psi_{s\alpha} \\ \Psi_{s\beta} \end{bmatrix} = \begin{bmatrix} L_m & 0 & M'x & -M'y \\ 0 & L_m & M'y & M'x \\ M'x & M'y & L_B & 0 \\ -M'y & M'x & 0 & L_B \end{bmatrix} \begin{bmatrix} i_{m\alpha} \\ i_{m\beta} \\ i_{s\alpha} \\ i_{s\beta} \end{bmatrix} \quad (4)$$

$$M' = \frac{\pi\mu_0 n_4 n_2 l}{8} \cdot \frac{r - (l_m + l_g)}{(l_m + l_g)^2}$$

$l$  = Length of rotor iron core

$l_m$  = Permanent magnet thickness

$l_g$  = Airgap length

$\mu_0$  = Magnetic conductance of air

The magnetic energy  $W_m$  stored in the windings can be written as

$$W_m = \frac{1}{2} \begin{bmatrix} i_{m\alpha} \\ i_{m\beta} \\ i_{s\alpha} \\ i_{s\beta} \end{bmatrix}^T \begin{bmatrix} L_M & 0 & M'x & -M'y \\ 0 & L_M & M'y & M'x \\ M'x & M'y & L_B & 0 \\ -M'y & M'x & 0 & L_B \end{bmatrix} \begin{bmatrix} i_{m\alpha} \\ i_{m\beta} \\ i_{s\alpha} \\ i_{s\beta} \end{bmatrix} \quad (5)$$

$$= \frac{1}{2} [i_{m\alpha}(L_m i_{m\alpha} + M'x i_{s\alpha} - M'y i_{s\beta}) + i_{m\beta}(L_m i_{m\beta} + M'y i_{s\alpha} + M'x i_{s\beta}) + i_{s\alpha}(M'x i_{m\alpha} + M'y i_{m\beta} + L_B i_{s\alpha} + i_{s\beta} - M'y i_{m\alpha} + M'x i_{m\beta} + L_B i_{s\beta})]$$

$$= \frac{1}{2} L_m (i_{m\alpha}^2 + i_{m\beta}^2) + \frac{1}{2} L_B (i_{s\alpha}^2 + i_{s\beta}^2) + M'x (i_{m\alpha} i_{s\alpha} + i_{m\beta} i_{s\beta}) + M'y (-i_{m\alpha} i_{s\beta} + i_{m\beta} i_{s\alpha})$$

$$\begin{bmatrix} F_x \\ F_y \end{bmatrix} = \begin{bmatrix} \frac{\delta W_m}{\delta x} \\ \frac{\delta W_m}{\delta y} \end{bmatrix} = M' \begin{bmatrix} i_{m\alpha} i_{\alpha'} + i_{m\beta} i_{\beta'} \\ -i_{m\alpha} i_{\beta'} + i_{m\beta} i_{\alpha'} \end{bmatrix} \quad (6)$$

$$= M' \begin{bmatrix} i_{m\alpha} & i_{m\beta} \\ i_{m\beta} & -i_{m\alpha} \end{bmatrix} \cdot \begin{bmatrix} i_{s\alpha} \\ i_{s\beta} \end{bmatrix}$$

The equation (4) and (5) are substituted into the equation (6). By substituting  $i_{m\alpha} = I_m \cos(2\omega t + \theta)$ ,  $i_{m\beta} = I_m \sin(2\omega t + \theta)$  and  $I_m = \sqrt{I_\alpha^2 + I_\beta^2}$  into equation (6) thus result the equation (7). This equation shows the relationship between radial suspension force and suspension winding current.

$$\begin{bmatrix} F_{mx} \\ F_{my} \end{bmatrix} = M' l_m \begin{bmatrix} \cos(2\omega t + \theta) & \sin(2\omega t + \theta) \\ \sin(2\omega t + \theta) & -\cos(2\omega t + \theta) \end{bmatrix} \begin{bmatrix} i_{s\alpha} \\ i_{s\beta} \end{bmatrix} \quad (7)$$

The stator flux linkage equation is shown as below

$$\begin{aligned} \Psi_{md} &= L_d i_d + \Psi_r \\ \Psi_{mq} &= L_q i_{mq} \end{aligned} \quad (8)$$

where  $\Psi_r$  is coupling flux linkage which rotor magnetically attractive in stator generates.  $L_\alpha$  and  $L_\beta$  are self inductance of motor windings. The equation for stator voltage equation is shown as (9).

$$\begin{aligned} V_{md} &= p\Psi_{md} - \omega\Psi_{mq} + r_1 i_d \\ V_{mq} &= p\Psi_{mq} + \omega\Psi_{md} + r_1 i_q \end{aligned} \quad (9)$$

Electromagnetic torque is consisting of electrical and mechanical torque equation written as (10). The mechanical torque equation is also been considered due to the impact of mechanical system on the drive performance.  $\tau_L$  is the external load torque,  $J$  is the moment of shaft inertia and  $D$  is the damping coefficient of viscous friction.

$$T_{em} = \frac{E i_q}{\omega_m} + \Psi_{mq} i_{mq} - \Psi_{md} i_{md} = J \frac{d\omega_m}{dt} + D\omega_m + \tau_L \quad (10)$$

### 3.2. Bearingless PMSM

The flowchart on designing bearingless PMSM is shown in Figure 2. The dimension of the motor design is summarized in Table 1. The parameters are inserted into RMxpert of FEM and then the model is converted into 2-Dimensional model. The result obtained from FEM shows the relationship of suspension current, rotor distance and force value at  $F_x$  and  $F_y$ .

Lastly, the controller for bearingless PMSM is designed by using Matlab to obtain the performance of motor through speed and to control the positions of rotor as shown in Figure 3. The subsystem for BPMSM is modelled by using the equation (3), (9) and (10) while force to current transformation is performed based on the equation (7). The proportional integral (PI) controller will amplify the difference between the detected displacement and the demand values of  $x^*$  and  $y^*$ . These allow the required radial suspension force,  $F_x^*$  and  $F_y^*$  can be correctly determined. To achieve the centre position, the value of  $x^*$  and  $y^*$  are set to 0. The results obtained from Matlab are force value, displacement value for  $x$  and  $y$  and speed.

Table 1. Parameter of bearingless PMSM

Parameter	Symbol	Value
Radius of stator inner surface	$r_s$	2.95mm
Radius of rotor iron core	$r_r$	14.91mm
Permanent magnet thickness	$l_m$	5.09mm
Airgap length	$l_g$	0.9595mm
Pole pair number of torque winding	$P_m$	2
Pole pair number of suspension force winding	$P_s$	1
Number of turns for motoring torque winding	$N_m$	54 turns
Number of turns for suspension force winding	$N_s$	54 turns

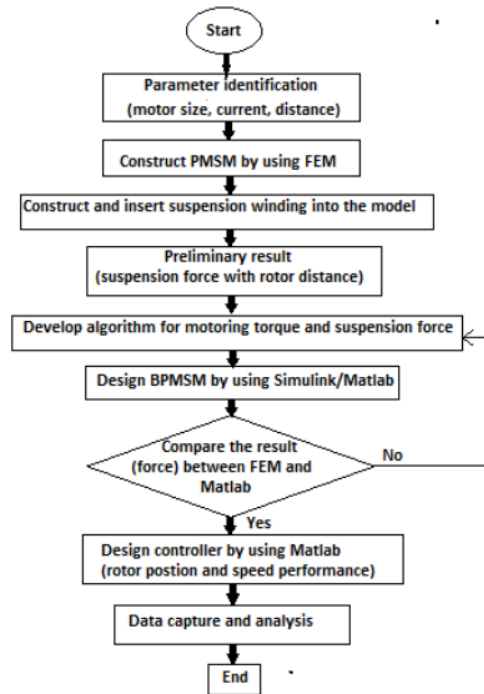


Figure 2. Project Flowchart

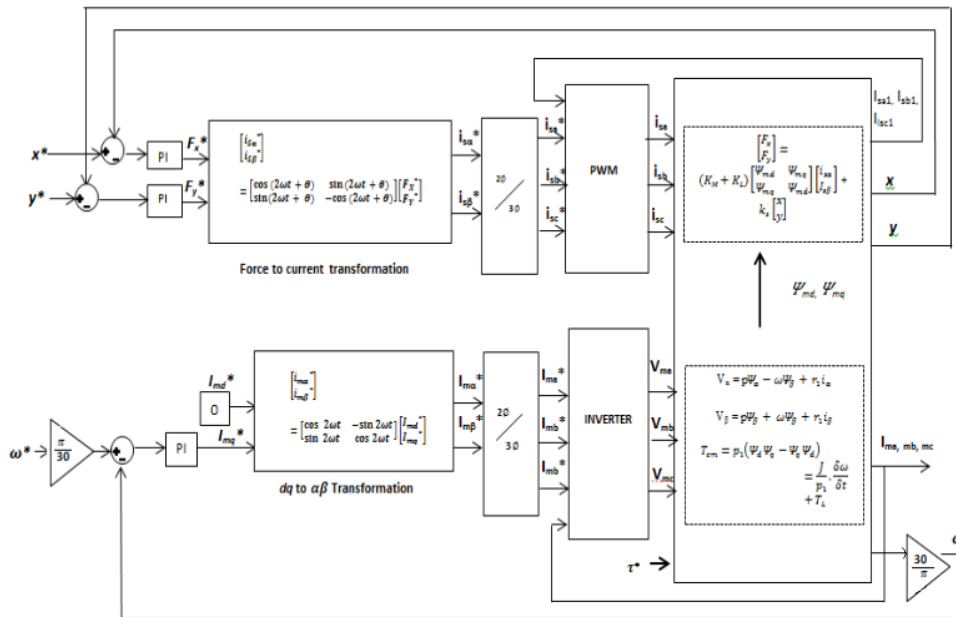


Figure 3. Control system of bearingless PMSM



**4. RESULTS AND ANALYSIS**

The simulation result is obtained from both simulation softwares which are FEM and Matlab/Simulink. The discussion for the result of independent suspension force motor and bearingless PMSM from FEM and Matlab is compared.

**4.1. FEM**

FEM is used in designing bearingless PMSM by using Ansys. The flux lines distribution in Figure 4 shows the results obtained before and after current supply. Figure 4 (a) shows the flux lines distribution is symmetrical with four pole fluxes when there is no current supply at motoring torque winding and voltage supply at suspension force winding. But when the source is supplied at phase *a* for windings, the flux lines distribution become unstable and focus at the right side.

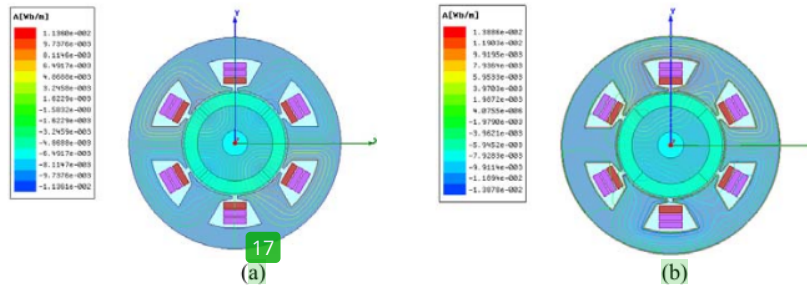


Figure 4. Flux lines distribution (a) before source supply and (b) after source supply

**4.2. Bearingless Permanent Magnet Synchronous Motor**

The result from FEM is proved by comparing it with the result from Matlab simulation. The comparison of force between these two simulations is shown in Figure 5 for independent suspension force model while Figure 6 is for bearingless PMSM model. From both figures, the graph lines of force value towards *x*-displacement between these two simulations are linear. The large difference for independent suspension force is below 18% while for bearingless PMSM, the difference force value is below 15%.

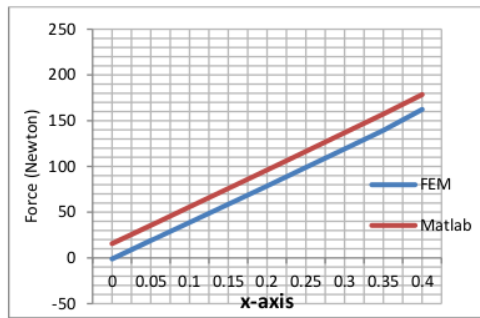


Figure 5. Comparison of FEM and Matlab for Independent suspension force model

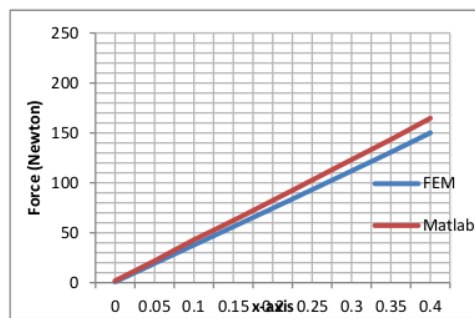


Figure 6. Comparison of FEM and Matlab for Bearingless PMSM

Then the result produced by digital control system is shown in the Figure 7 which displays the performance of rotor movement. The parameter used for rated speed is 1500 rpm, stator resistance is 1.4 Ω, moment of inertia *J* is 0.00176 kg.m<sup>2</sup>, stator inductance *L<sub>d</sub>* and *L<sub>q</sub>* are 0.0066 H and 0.0058 H. Based on the reference value, the rotor will be levitated and maintained at 0mm for both displacement values. Initially the rotor at -*x* and *y*-displacement is unstable and the oscillation is higher at first because of the speed oscillation.

However, the oscillation of rotor is still acceptable and the rotor does not touch the inner stator. As the speed reaches the reference speed at 0.05s, the rotor displacement is stable and maintained at zero on both  $x$ - and  $y$ -displacements. Although the rotor movement maintains at zero position but there is still small vibration occurred which is around  $0.02\mu$  for  $x$ -displacement and  $0.1\mu$  for  $y$ -displacement.

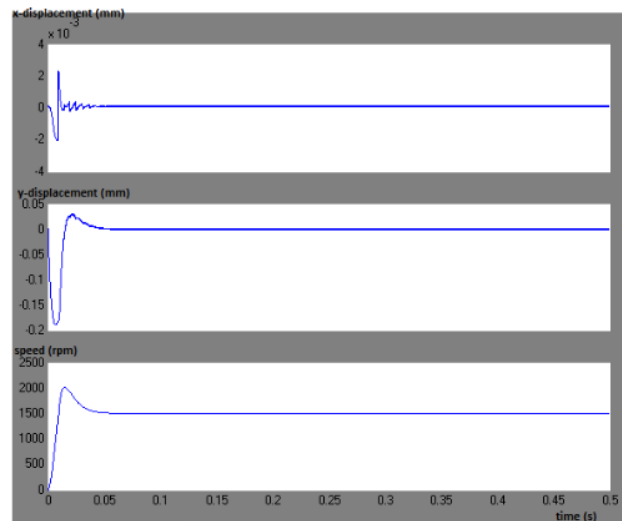


Figure 7. Waveform at  $x$  and  $y$ -displacement with speed performance

The test of the motor controller is conducted by setting the displacement demand value for  $x^*$  which is set to 0.25mm and 0.3mm while  $y^*$  is maintained at 0. A figure 8 show the rotor is oscillated high at below 0.05s due to the speed performance does not achieve its steady state condition. But after the speed waveform reaches the rated speed value, the  $x$ -displacement value is maintained at the reference position.

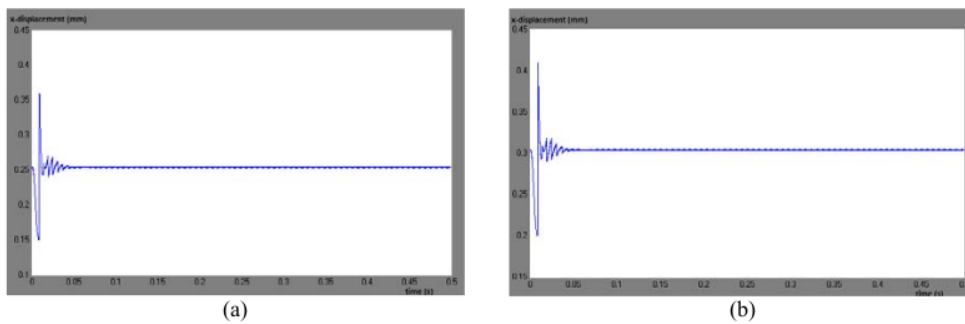


Figure 8. Rotor radial displacement at (a) 0.25mm (b) 0.3mm



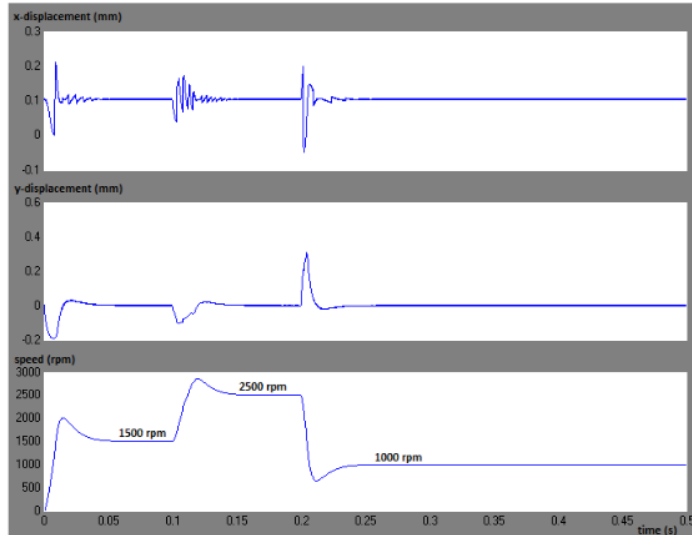


Figure 9. Rotor suspension test when speed is increase and decrease

The test of the rotor radial displacement towards the rotor speed is conducted in order to see the effect of rotor moment when the speed varies by increasing and decreasing the speed value. As shown in the Figure 9, the speed is increased from 1500 rpm to 2500 rpm and then decreased to 1000 rpm. The changes of the speed values give the effect to the rotor performance. The reference  $x$ -displacement value is set to 0.1mm. It can be seen that when the speed is increased from 1500 rpm to 2500 rpm the radial displacements for  $x$  and  $y$  are oscillating during speed overshoot period. However, as soon as they reach the reference speed, the rotor radial displacements maintain regulated back at reference position. The same condition is occurring when the speed is decreased from 2500 rpm to 1000 rpm. The oscillations at  $x$  and  $y$  displacement are higher when the speed drops but maintain after reach the reference speed.

## 5. CONCLUSION

The research on designing the model of bearingless PMSM is to find the suitable mathematical model to levitate and rotate the rotor component depending on the magnet attraction towards windings. There are two main mathematical models which are motoring torque equation and radial suspension force equation. Two methods are proposed which is by independent suspension model and another one is general bearingless PMSM. The surface mount permanent magnet is used in this paper by designing the model using FEM simulation 2-Dimensional and Matlab/Simulink. The experimental setup for this BPMSM will be performed later to further improve both model and control algorithm.

## ACKNOWLEDGEMENTS

The authors would like to thank to the Universiti Teknikal Malaysia Melaka (UTeM) for providing FRGS/2012/FKE/TK02/1/F00113 and FRGS/2/2013/TK02/FKE/02/2/F00168

## REFERENCES

- [1] X. Sun, et al., "Overview of Bearingless Permanent Magnet Synchronous Motors", *IEEE Journal of Jiangsu University*, pp. 2-11, 2011.
- [2] N. Zhong-jin, et al., "Magnetic Field Analysis of Bearingless Permanent Magnet Motor", *IEEE Journal of Zhejiang University*, pp. 450-453, 2011
- [3] H. Zhu, et al., "Mathematical Model and Control Technology of Bearingless PMSM", *IEEE Chinese Control and Decision Conference*, pp. 143-3179, 2010
- [4] J. Deng, et al., "Digital Control System on Bearingless Permanent Magnet-type Synchronous Motors", *IEEE Journal of Jiangsu University (Electrical and Information Engineering)*, February 7, 2006

- [5] F. Liang, *et al.*, "Digital Control System on Bearingless Permanent Magnet Synchronous Motor", *IEEE Journal of Zhejiang University*, pp.4040-4043, 2011.
- [6] Y. Lv, *et al.*, "Modelling and Digital Control System for Bearingless Permanent Magnet Synchronous Motor Based on Magnetic Energy Equation", *International conference on Electrical Machines and Systems (ICEMS)*, 2011.
- [7] W. Qiaoqiao, *et al.*, "Force Analysis of a Bearingless Permanent Magnet synchronous Motor", *IEEE 3<sup>rd</sup> International Symposium on IITA*, pp.495-498, 2009
- [8] M. Ooshima, *et al.*, "Characteristics of a permanent magnet type bearingless motor", *IEEE Trans. Indus. Application*, vol. 32, pp. 292-299, April 1996
- [9] M. Henzel and K. Falkowski, "The analysis of the Bearingless Electric Motor with Surface-mounted Permanent Magnets", *IEEE Journal of Military University of Technology*, pp. 215-220, 8 12
- [10] X. Ye, *et al.*, "Research for the Design Scheme of Bearingless Motors", *International Conference on Electrical Machines and Systems, Wuhan, China*, pp. 208-211, Oct 2008
- [11] A. Chiba, *et al.*, "Magnetic Bearings and Bearingless Drives", Amsterdam, The Netherlands: Elsevier, Mar. 2005
- [12] H. Zhu, *et al.*, "Modelling of Bearingless Permanent Magnet Synchronous Motor Based on Mechanical to Electrical Coordinates Transformation", *Sci. China Ser. 2* vol.52. no.12, pp.3736-3744, Dec. 2009
- [13] M. Ooshima, *et al.*, "Characteristics of a permanent Magnet type Bearingless Motor", *IEEE Trans. Indus. Application*, vol. 32, pp. 6 2-299, 1996
- [14] H. Zhu and T. Zhang, "Finite Element Analysis for Bearingless Permanent Magnet-Type Synchronous Motor", *Proceeding of the CSEE*, Vol. 26, No. 3, pp. 136-140, 2006
- [15] G. Munteanu, *et al.*, "No-load Tests of a 40kW high-speed Bearingless Permanent Magnet Synchronous Motor", *Proc. Int. Sym. Power Electron. Elect. Drive Autom. Motion*, pp. 1460-1465, 2010

# Bearingless Permanent Magnet Synchronous Motor using Independent Control

---

ORIGINALITY REPORT

---

7%

SIMILARITY INDEX

---

PRIMARY SOURCES

---

- 1 Huimin Zhu, Zebin Yang, Xiaodong Sun, Ding Wang, Xi Chen. "Rotor Vibration Control of a Bearingless Induction Motor Based on Unbalanced Force Feed-Forward Compensation and Current Compensation", IEEE Access, 2020  
51 words — 2%  
Crossref
- 2 Huangqiu Zhu, Jianbo Huang. "Compensation control of suspension force for LS-BLPMMSM", IET Electric Power Applications, 2017  
17 words — 1%  
Crossref
- 3 Sun, X., S. Luo, J. Zhu, Z. Yang, and F. Li. "Modeling of a bearingless permanent magnet synchronous motor using adaptive weighted least square support vector machine", 2015 IEEE Magnetics Conference (INTERMAG), 2015.  
15 words — < 1%  
Crossref
- 4 [www.slideshare.net](http://www.slideshare.net)  
Internet  
11 words — < 1%
- 5 Akcayol, M.A.. "NEFCLASS-based neuro fuzzy controller for SRM drive", Engineering Applications of Artificial Intelligence, 200508  
10 words — < 1%  
Crossref
- 6 [caod.oriprobe.com](http://caod.oriprobe.com)  
Internet

10 words — < 1%

7 gsse.ku.edu.tr  
Internet

10 words — < 1%

8 Publications

9 words — < 1%

9 Z. Tao. "Comparison and analysis of bearingless permanent magnet synchronous motor with different magnetized rotor", 2017 IEEE International Magnetics Conference (INTERMAG), 2017  
Crossref

9 words — < 1%

10 www.scitechnol.com  
Internet

9 words — < 1%

11 COMPEL: The International Journal for Computation and Mathematics in Electrical and Electronic Engineering, Volume 33, Issue 1-2 (2014-03-28)  
Publications

8 words — < 1%

12 T. Fukao. "An identification method of suspension force and magnetic unbalance pull force parameters in buried-type IPM bearingless motors", IEEE Power Engineering Society General Meeting 2004 PES-04, 2004  
Crossref

8 words — < 1%

13 ceria.utem.edu.my  
Internet

8 words — < 1%

14 oriprobe.com  
Internet

8 words — < 1%

15 studentsrepo.um.edu.my  
Internet

8 words — < 1%

16 Masahide Ooshima. "Compensation Method of Radial Unbalance Force at Failure of a Motor Section in a d-q Axis Current Control Bearingless Motor", 2018 International Power Electronics Conference (IPEC-Niigata 2018 - ECCE Asia), 2018  
7 words — < 1%  
Crossref

---

17 Widyan, Mohammad S.. "Design, Optimization, Construction and Test of Rare-Earth Permanent-Magnet Electrical Machines with New Topology for Wind Energy Applications", Technische Universität Berlin, 2006.  
7 words — < 1%  
Publications

---

18 Yukun Sun, Fan Yang, Ye Yuan, Yonghong Huang. "Out rotor bearingless brushless DC motor for flywheel energy storage", 2017 International Workshop on Complex Systems and Networks (IWCSN), 2017  
6 words — < 1%  
Crossref

---

EXCLUDE QUOTES OFF  
EXCLUDE BIBLIOGRAPHY OFF

EXCLUDE MATCHES OFF